

## Nonlinear Behavior of Self -Compacting Reinforced Concrete Two-Way Slabs with Central Square Opening under Uniformly Distributed Loads

Dr. Ali Hussein Ali Al-Ahmed

Lecturer

College of Engineering - University of Baghdad-

ali\_hussein\_alahmed@yahoo.co.uk

### ABSTRACT

This research is carried out to investigate the behavior of self-compacting concrete (SCC) two-way slabs with central square opening under uniformly distributed loads. The experimental part of this research is based on casting and testing six SCC simply supported square slabs having the same dimensions and reinforcement. One of these slabs was cast without opening as a control slab. While, the other five slabs having opening ratios ( $O_R$ ) of 2.78%, 6.25%, 11.11%, 17.36% and 25.00%. From the experimental results it is found that the maximum percentage decrease in cracking and ultimate uniform loads were 31.82% and 12.17% compared to control slab for opening ratios ( $O_R$ ) of 11.11% and 6.25% respectively. Also the results showed that as  $O_R$  is increased from 0.00% to 11.11%, a significant increase in deflection was occurred. While the increase of  $O_R$  from 11.11% to 25.00%, a slightly decrease in deflection was occurred compared to control slab within the entire range of loading starting from first cracking load up to ultimate load. The theoretical part of this research is adopted for both simply supported and clamped ends square slabs according to yield line theory. For simply supported slabs, the results showed a decrease in ultimate uniform loads for  $O_R$  ranging between 0.00% and 25.00%. While beyond this value, an increase in the ultimate uniform load is occurred. In addition, it is found that as  $O_R$  was increased; the total ultimate load is decreased. Also from the theoretical analysis for clamped end slabs it is found that as  $O_R$  was increased, both the ultimate uniform load and the total ultimate load were increased.

**Key words:** self-compacting concrete, square opening, two-way slabs, yield lines, uniform load

### التصرف اللاخطي للبلاطات الخرسانية المسلحة ذاتية الرص العاملة باتجاهين ذات فتحات مربعة في المركز تحت تأثير احمال منتشرة

د. علي حسين علي آل احمد

مدرس

جامعة بغداد-كلية الهندسة

### الخلاصة

في هذا البحث تم التحري عن تصرف البلاطات الخرسانية المسلحة ذاتية الرص العاملة باتجاهين ذات فتحات مربعة في المركز تحت تأثير احمال منتشرة منتظمة. تضمن الجانب العملي من هذا البحث صب وفحص ستة بلاطات خرسانية ذاتية الرص مربعة الشكل ذات اسناد بسيط لها نفس الابعاد وحديد التسليح. كانت احدى هذه البلاطات بدون فتحة حيث اتخذت كبلطة مرجعية للمقارنة. بينما احتوت البلاطات المتبقية على فتحات مربعة في المركز بنسب ( 2.78%، 6.25%، 11.11%، 17.37% و 25.00%) من المساحة السطحية للبلاطة. وجد من النتائج العملية ان اكبر نسبة نقصان في حمل التشقق والحمل الاقصى المنتشر كان 31.82% و 12.17% لنسب فتحات 11.11% و 6.25% على التوالي مقارنة مع البلاطة المرجعية. كذلك اظهرت النتائج ان بزيادة نسبة الفتحة من 0.00% الى 11.11% حدثت زيادة في الهطول في حين ان زيادة نسبة الفتحة من 11.11% الى 25.00% ادت الى نقصان في الهطول مقارنة مع البلاطة المرجعية ضمن منطقة التصرف ابتداء من حمل التشقق الى الحمل الاقصى المنتشر. تبني الجانب النظري من هذا البحث نظرية خطوط الخضوع



لتحليل بلاطات ذات اسناد بسيط واخرى مقيدة الحافات. للبلاطات ذات الاسناد البسيط وجد بان هنالك نقصان في الحمل الاقصى المنتشر لنسبه فتحات تتراوح من % 0.00 الى % 25.00. بينما بعد هذه النسبة حدثت زيادة في قيمة الحمل الاقصى المنتشر. وجد كذلك ان زيادة نسبة الفتحة ادى الى نقصان في قيمة الحمل الكلي. اما بالنسبة للبلاطات مقيدة الحافات فوجد بان زيادة نسبة الفتحات ادى الى زيادة في القيم القصوى للاحمال المنتشرة والاحمال الكلية سوية.

**الكلمات الرئيسية:** خرسانة ذاتية الرص، فتحات مربعة، بلاطات عاملة باتجاهين، خطوط الخضوع، احمال منتشرة منتظمة

## 1. INTRODUCTION

Reinforced concrete (RC) slabs are the most common elements in structural buildings and have been widely used for multi-storey buildings. Openings are often required in slabs for mechanical and electrical services such as heating, plumbing, electrical wiring, fire protection pipes, telephone, computer network, water supply, sewerage and ventilating reasons. Meanwhile, substantial size openings are required by lift, staircases and elevator shafts. The structural effect of small openings is usually not considered due to ability of the structure to redistribute the stresses. However, for large openings in slabs can severely reduce the strength and load carrying capacity of these slabs due to cut out of both concrete and steel reinforcement. This may lead to decrease the ability of structures to withstand the imposed loads and the structural needs, **Taljsten et. al, 2006; Mota, and Kamara, 2006.**

Two- way RC slab is a form of unique construction of reinforced concrete. It is an efficient, economic and widely used member. It is usually supported by all four sides and the ratio of long span to short span is less than two. So that, two- way RC slab will deflect in two directions and the loads are transferred to all supports. In general there are three types of RC two- way slabs: flat plates, flat slab and slab supported on beams, **Wang et. al, 2007.**

Self-Compacting Concrete (SCC) is an innovative concrete flows under its own weight and it does not require any external vibration for compaction. It was first developed in the late 1980's by Japanese researchers. SCC can flow through restricted sections without segregation and bleeding and completely filling formwork and achieving full compaction. Such concrete should have a relatively low yield value to ensure high flow ability, a moderate viscosity to resist segregation and bleeding, **Nagamoto, and Ozawa, 1997 and Khayat, and Ghezal, 1999.**

## 2. STRUCTURAL DESIGN OF REINFORCED CONCRETE SLABS WITH OPENINGS

The design of RC slab with openings is not clearly declared in the **BS 8110, 1997.** However, the **ACI 318, 2014** Code states that the openings are permitted in new slab system. The ACI Code provides guide lines for different location of openings in RC flat slabs. **Fig. 1** illustrates the openings size and their locations in flat slab. The flat slab is divided into column and middle strips in two orthogonal directions. The ACI Code suggests that any size of opening is permitted in the area of where middles strip intersects. For opening in the area intersecting column strip, the permissible opening size is only 1/8 the width of column strip in either span directions. Finally, for opening in the area that intersecting one column strip and one middle strip, the maximum permissible opening size is only 1/4 the width of column or middle strip in either span directions.

## 3. EXPERIMENTAL PROGRAM

### 3.1 Introduction

The main purpose of the experimental work is to investigate the behavior of SCC two-way slabs with central square opening under uniformly distributed load. The primary variable in this research is the opening ratio ( $O_R$ ) which is equal to the area of opening divided by the area of solid slab multiplied by 100.



The standard tests were carried out to determine the properties of hardened concrete and steel reinforcement. In addition, instrumentation, experimental setup and testing procedures adopted throughout this investigation are presented.

### 3.2 Specimens

The experimental work is based on casting and testing six SCC square slabs. All specimens have the same dimensions of (650×650×50 mm) were cast and tested up to failure under a uniform load. The slabs are designed as simply supported along four edges and supported on the (600×600 mm) perimeter at the bottom side of the slabs. One of these slabs was without opening (solid) which is taken as a control slab and denoted as S-0. While the other five slabs have different square openings located at the center of slab. Five openings with dimensions (100 x 100, 150 x 150, 200 x 200, 250 x 250 and 300 x 300 mm) were created at the center of the slabs, so that the opening ratios ( $O_R$ ) were (2.78%, 6.25%, 11.11%, 17.36% and 25.00%) respectively. These slabs are denoted as S-10, S-15, S-20, S-25 and S-30 for the above opening ratios ( $O_R$ ) as listed in **Table 1**.

All specimens were reinforced at bottom with  $\phi$  2.5 mm @ 50 mm steel bars in both directions with effective depth ( $d$ ) of 40 mm, so that the steel ratio ( $\rho$ ) is about 0.245% which lies within the ACI Code limits. Also, each corner of the openings was provided with  $2\phi$ 2.5 mm additional diagonal steel bars to prevent stress concentration. Full details of the test slabs are shown in **Fig. 2**.

### 3.3 Material Used for Casting Specimens

#### 3.3.1 Cement

Ordinary Portland cement type (I) was used throughout this investigation. All quantity of cement was tested chemically and physically. The properties were conform to the **Iraqi Specifications No. 5, 1984**. for Portland cement.

#### 3.3.2 Fine and coarse aggregate

Natural sand from Al-Akhaidher quarries was used for SCC mixes. The fine aggregate has (4.75mm) maximum size with rounded-shape particles and smooth texture. While, crushed gravel from Al-Sudor region with maximum size of 10 mm was used throughout this research. The sand and gravel have been washed and cleaned with water several times and they were conform to the **Iraqi specification No.45, 1984**.

#### 3.3.3 Limestone powder

To produce SCC, crushed limestone powder (LSP) was used in this investigation. This LSP is passed sieve No. 0.075 mm and tested physically and chemically.

#### 3.3.4 Superplasticizer

Glenium 51 was used in this research as a superplasticizer material to produce SCC. Glenium 51 is free of chlorides and it was conform to **ASTM C494** type A and F.

#### 3.3.5 Steel bars

$\phi$  2.5 mm plain steel bars were used for reinforcement. For these bars, yield stress ( $f_y$ ) and ultimate strength ( $f_u$ ) were 590 MPa and 690 MPa respectively. While, the modulus of elasticity ( $E_s$ ) was 205000 MPa.

### 3.4 Molds Fabrication

In the present research, six molds were used to cast the specimens. These molds were made from plywood plates (18 mm) thickness and had a base and four sides to form a square frame. In addition, five square wooden frames with different opening sizes are fabricated and located at the center of each slab to form the opening size required. Before casting the SCC, these molds were oiled and the reinforcement meshes were put into the required position as shown in **Fig. 3**.

### 3.5 Mix Design

In the present research, SCC was used for casting the specimens. After several trial mixes according to recommendations mentioned in **The European Guidelines for Self-Compacting Concrete, 2005**, concrete mixture was designed to achieve a cylindrical compressive strength ( $f_c$ ) of 30 MPa at 28 days. **Table 2** illustrates the mix design properties of SCC used in this investigation.

### 3.6 Test Rig Components and Loading Procedure

In the present research, the hydraulic testing machine at the Civil Engineering Department Lab. of the University of Baghdad was used. All specimens were white painted to facilitate the identification of cracks during the test. All test slabs were mounted on a supporting frame which have a 30 mm bar welded along each side at the upper of supporting frame to achieve simply supported condition. Several dial gauges were used in this investigation and attached the tension face of slabs. These dial gauges were located at distances of (150, 175, 200, 225, 250 and 300 mm) measured from supports for control slab (S-0). While for slabs with opening, one or more dial gauges were excluded according to opening size condition as illustrated in **Table 3**.

To apply a uniformly distributed load on slabs, an aluminum sand container was put on the top face of specimens and filled with sand. A steel plate with dimensions of (550 x 550 x 15 mm) was put on sand. Also a steel block of dimensions (550 x 450 x 50 mm) was put on steel plate to insure full distribution of load on specimens. Hydraulic jack and load cell were put respectively on steel block. The weight of sand, steel plate, steel block, hydraulic jack and load cell were taken into account and added to external applied load. **Fig. 4** shows full details of test rig components and setup of a typical tested slab.

The specimens were uniformly loaded with increasing load until failure. At each load step, deflections reading by dial gauges were recorded.

## 4. EXPERIMENTAL RESULTS

All beams were tested up to failure by applying uniformly distributed load with load division of (10 kN/m<sup>2</sup>) for steps before cracking. While for steps after cracking, the load division was reduced to (2.5 kN/m<sup>2</sup>).

### 4.1 Cracking and Ultimate Loads Results

All slabs are characterized by the formation of cracks at the tension face of slabs and yield lines propagated from corner of opening toward corner of supports till failure occur. **Fig. 5** shows tested slabs after forming yield lines and failure. From this figure it could be noticed that for slabs S-0, S-10 and S-15 only diagonal yield lines were occurred. While, for slabs S-20, S-25 and S-30 additional straight cracks were developed perpendicular to the sides of openings. This might be due large opening size effect. The experimental results for cracking and ultimate uniform loads of all specimens are given in **Table 4**. From this table it could be noticed that the control slab S-0 had maximum cracking and ultimate load capacities. The cracking and ultimate uniform loads were decreased as  $O_R$  was increased from 0.00% to 25.00%. The maximum



percentage decrease in cracking load was 31.82% for slab S-20 ( $O_R=11.11\%$ ) compared to control slab. Beyond this value of  $O_R$ , the percentage decrease in cracking load was decreased as  $O_R$  was increased from 11.11% to 25.00%.

The maximum percentage decrease in ultimate uniform load was 12.17% for slab S-15 ( $O_R=6.25\%$ ) compared to control slab. Beyond this value of  $O_R$ , the percentage decrease in ultimate uniform load was decreased when  $O_R$  was increased from 6.25% to 25.00%. For slab S-30 ( $O_R=25.00\%$ ), the ultimate load capacity is approximately similar to value obtained from control slab. This might be due concentration of the uniform load near supports and increasing slab stiffness. **Fig. 6** shows the percentage decrease in cracking and ultimate uniform loads with increasing opening ratio ( $O_R$ ).

Cracking to ultimate load ratios ( $w_{cr}/w_u$ ) were also calculated and listed in **Table 4**. The maximum and minimum ( $w_{cr}/w_u$ ) ratios are 0.507 and 0.386 for slab S-0 (control) and S-20 ( $O_R=11.11\%$ ) respectively.

#### 4.2 Load-Deflection Response

Deflections for each slab have been recorded during the test by using dial gauges located at the positions listed in **Table 3**. **Fig. 7** shows the load-deflection response for each tested slab at different dial gauge locations (i.e variable dial gauge locations with constant  $O_R$ ). From this figure it could be noticed that a linear behavior of the load-deflection response is evident. This stage covers the region up to the cracking load. Within this stage the materials are still elastic and no cracks occur in the specimens. When cracks have taken place, a sudden jump in deflection value was occurred. Those cracks are developed as the load increases and the response changes from linearity to nonlinearity because the rate of increase in deflection with respect to load continuously increases as the load is increased and the curve behaved nonlinearly as load increased. Finally as the applied load approaches its ultimate value, the rate of increase in deflection is substantially exceeding the rate of increase in the value of applied load till failure occurred. Also it is clear from this figure that for each tested slab, the deflection is increased as the location of dial gauge is far from supports.

**Fig. 8** shows the load-deflection response for each tested slab recorded by same dial gauge location (i.e constant dial gauge location with variable  $O_R$ ). It is clear from this figure that the increase in  $O_R$  has a significant effect on deflection through the entire range of loading starting from cracking load up to ultimate uniform load. For slabs S-10, S-15 and S-20 of  $O_R$  (2.78%, 6.25% and 11.11%) respectively, the load-deflection curve showed a significant increase in deflection values compared to control slab. While for slabs S-25 and S-30 with  $O_R$  of (17.36% and 25.00%) respectively, the load-deflection curve showed a slightly decrease in deflection values compared to control slab. This is might be due to the effect of large opening size on shifting the concentration of the uniform load towards the supports and that will make the slab stiffer.

To obtain a reasonable comparison of deflections among tested slabs, **Table 5** summarizes the deflection recorded at different locations corresponding to a load level of 130 kN/m<sup>2</sup> which is about 85% of ultimate uniform load capacity of the control slab. Also **Fig. 9** shows the percentage increase and decrease in deflection with respect to distance of recorded deflection from supports for different values of  $O_R$ . While, **Fig. 10** shows the percentage increase and decrease in deflection with respect to  $O_R$  for different values of distances from supports. From these figures and **Table 5**, it may be noticed that the maximum percentage increase in deflection is 39.13% for slab S-10 ( $O_R=2.78\%$ ) at location of 250 mm from supports. While, the maximum percentage decrease in deflection is 11.47% for slab S-25 ( $O_R=17.36\%$ ) at location of 175 mm from supports corresponding to a load level of 130 kN/m<sup>2</sup>.



## 5. THEORETICAL ANALYSIS USING THE YIELD LINE THEORY

Simply supported and clamped ends square slabs with central square opening as shown in **Fig.11** were considered in this theoretical analysis. These slabs are considered to have isotropic reinforcement (i.e  $m_x = m_y$ ). Yield lines are assumed to propagate from the corner of opening toward the corner of slab. Also, these slabs are subjected to a uniformly distributed load ( $w$ ) and a unit displacement ( $\Delta=1$ ) is applied at the edge of opening.

### 5.1 Case-1 Simply Supported Slab

According to **Fig. 11-a**, the external work ( $WE$ ) done by the applied load is given by Eq. (1)

$$WE = w_u (\text{slab with opening}) \times 4 \left\{ \left( Z \times \frac{(L-Z)}{2} \times \frac{1}{2} \right) + \left( \left( \frac{1}{2} \times (L-Z) \times \frac{(L-Z)}{2} \times \frac{1}{3} \right) \right) \right\}$$

$$WE = w_u (\text{slab with opening}) \left\{ \frac{(L-Z)(L+2Z)}{3} \right\} \quad (1)$$

where:

$L$  = dimension of square slab.

$Z$  = dimension of central square opening.

If the positive resistance moment per unit length along the yield lines is defined as ( $m$ ), the internal work ( $WI$ ) done by this moment is given by Eq. (2)

$$WI = 4ml\theta$$

$$WI = 4m \times (L - Z) \times \frac{1}{\frac{(L-Z)}{2}}$$

$$WI = 8m \quad (2)$$

where:

$l$  = projected length of the yield line.

$\theta$  = rotation along the yield line.

Equating the external work with the internal work gives Eq. (3) which represents the relation between ( $w$ ) and ( $m$ ) for case of simply supported slab with opening. Multiplying Eq. (3) by the area of slab ( $L^2-Z^2$ ) gives Eq. (4) which represents the relation between total load ( $P$ ) and ( $m$ ) for the same case.

$$w_u (\text{slab with opening}) = \frac{24 m}{(L-Z)(L+2Z)} \quad (3)$$

$$P_u (\text{slab with opening}) = \frac{24 m (L+Z)}{(L+2Z)} \quad (4)$$

If  $Z=0$  (solid slab) then Eq. (3) gives Eq. (5) which represents the relation between ( $w$ ) and ( $m$ ) for case of simply supported solid slab. While, Eq. (4) gives Eq. (6) which represents the relation between ( $P$ ) and ( $m$ ) for the same case.

$$w_u (\text{solid slab}) = \frac{24 m}{L^2} \quad (5)$$

$$P_u (\text{solid slab}) = 24m \quad (6)$$

Hence, the ratio of ultimate uniform load for a slab with opening to ultimate uniform load for a solid slab ( $UL_R$ ) is given by Eq. (7). This equation is obtained when Eq. (3) is divided by Eq. (5). While, the ratio of total ultimate load for a slab with opening to total ultimate load for a solid slab ( $TL_R$ ) is given by Eq. (8) when Eq. (4) is divided by Eq. (6).



$$UL_R = \frac{w_u (\text{slab with opening})}{w_u (\text{solid slab})} = \frac{L^2}{(L-Z)(L+2Z)} \quad (7)$$

$$TL_R = \frac{P_u (\text{slab with opening})}{P_u (\text{solid slab})} = \frac{(L+Z)}{(L+2Z)} \quad (8)$$

Since, area of solid slab= $L^2$ , area of opening= $Z^2$  and % Opening ratio ( $O_R$ ) =  $\frac{\text{Area of opening}}{\text{Area of solid slab}} \times 100$  so that Eqs. (7 & 8) can be expressed by Eqs. (9 & 10) respectively.

$$UL_R = \frac{w_u (\text{slab with opening})}{w_u (\text{solid slab})} = \frac{1}{(1 - \frac{\sqrt{\%O_R}}{10})(1 + \frac{\sqrt{\%O_R}}{5})} \quad (9)$$

$$TL_R = \frac{P_u (\text{slab with opening})}{P_u (\text{solid slab})} = \frac{(1 + \frac{\sqrt{\%O_R}}{10})}{(1 + \frac{\sqrt{\%O_R}}{5})} \quad (10)$$

By using Eqs. (9 & 10), **Figs. 12 and 13** are plotted to represent the effect of  $O_R$  on the  $UL_R$  and  $TL_R$  values respectively for simply supported square slabs. From **Fig. 12** it can be noticed that for  $O_R$  ranging between 0.00% to 25.00% the slabs with opening showed decreasing values of ultimate uniform load with respect to solid slab. The maximum decrease in  $UL_R$  is 0.889 occurred when  $O_R=6.25\%$ . This value is in agreement with the results obtained from the experimental test for slab S-15 ( $O_R=6.25\%$ ). Also **Fig. 12** shows that beyond  $O_R$  of 25.00%, a significant increase in the ultimate uniform load is occurred. This might be due to concentration of uniform load near supports for large opening ratios. So that larger load is needed for the external work to achieve equilibrium with the internal work. For  $O_R=60\%$ , the ultimate uniform load is about 1.75 times the uniform load of solid slab. From **Fig. 13** it can be noticed that as  $O_R$  is increased, the  $TL_R$  is decreased. For  $O_R=25\%$  and 60%, the total ultimate loads are 0.750 and 0.696 of total ultimate load of the solid slab respectively. It can be also noticed from **Fig. 13** that beyond  $O_R$  of 25.00%, a continuous decrease in  $TL_R$  is occurred which is unlike the behavior of  $UL_R$  noticed from **Fig. 12**.

**Table 6** summarizes the experimental and the theoretical values of  $UL_R$  and  $TL_R$ . This table show good agreement between the experimental and theoretical results.

## 5.2 Case-2 Clamped Ends Slab

According to **Fig. 11-b**, the external work done by the applied load is also given by Eq. (1) obtained for simply supported slab.

If ( $\beta$ ) is defined as the ratio of the negative resistance moment at clamped ends to the positive resistance moment along the positive yield lines, the internal work done by these moments is given by Eq. (11)

$$\begin{aligned} WI &= 4ml\theta + 4\beta mL\theta \\ WI &= 4m \times (L - Z) \times \frac{1}{\frac{(L-Z)}{2}} + 4\beta m \times L \times \frac{1}{\frac{(L-Z)}{2}} \\ WI &= 8m \left( \frac{L-Z+\beta L}{L-Z} \right) \end{aligned} \quad (11)$$

Equating the external work given by Eq. (1) with the internal work given by Eq. (11) gives Eq. (12) which represents the relation between ( $w$ ) and ( $m$ ) for clamped ends slab with central



opening. Total load ( $P$ ) is given by Eq. (13) which is also adopted by multiplying Eq. (12) by the area of slab ( $L^2-Z^2$ ).

$$W_u (\text{slab with opening}) = \frac{24 m(L-Z+\beta L)}{(L-Z)^2(L+2Z)} \tag{12}$$

$$P_u (\text{slab with opening}) = \frac{24 m(L-Z+\beta L)(L+Z)}{(L-Z)(L+2Z)} \tag{13}$$

If  $Z=0$  (solid slab) then Eq. (12) gives Eq. (14) which represents the relation between ( $w$ ) and ( $m$ ) for solid clamped ends slab. While, Eq. (13) gives Eq. (15) which represents the relation between ( $P$ ) and ( $m$ ) for solid clamped ends slab.

$$W_u (\text{solid slab}) = \frac{24 m(1+\beta)}{L^2} \tag{14}$$

$$P_u (\text{solid slab}) = 24m (1 + \beta) \tag{15}$$

Hence, the expression for  $UL_R$  and  $TL_R$  is given by Eqs. (16 & 17) respectively.

$$UL_R = \frac{W_u (\text{slab with opening})}{W_u (\text{solid slab})} = \frac{L^2(L-Z+\beta L)}{(L-Z)^2(L+2Z)(1+\beta)} \tag{16}$$

$$TL_R = \frac{P_u (\text{slab with opening})}{P_u (\text{solid slab})} = \frac{(L-Z+\beta L)(L+Z)}{(L-Z)(L+2Z)(1+\beta)} \tag{17}$$

Also similar to Eqs. (7 and 8), Eqs. (16 and 17) can be expressed by Eq. (18 & 19).

$$UL_R = \frac{W_u (\text{slab with opening})}{W_u (\text{solid slab})} = \frac{1 - \frac{\sqrt{\%O_R}}{10} + \beta}{(1+\beta)(1 - \frac{3(\%O_R)}{100} + \frac{\%O_R \sqrt{\%O_R}}{500})} \tag{18}$$

$$TL_R = \frac{P_u (\text{slab with opening})}{P_u (\text{solid slab})} = \frac{(1 - \frac{\sqrt{\%O_R}}{10} + \beta)(1 + \frac{\sqrt{\%O_R}}{10})}{(1+\beta)(1 - \frac{\sqrt{\%O_R}}{10})(1 + \frac{\sqrt{\%O_R}}{5})} \tag{19}$$

**Figs. 14 and 15** are plotted by using Eqs. (18 & 19). These figures show the effect of  $O_R$  on the  $UL_R$  and  $TL_R$  respectively for clamped end slabs for different values of  $\beta$ . From these figures it could be noticed that as  $O_R$  is increased, both  $UL_R$  and  $TL_R$  are increased for all values of  $\beta$  except ( $\beta=0.5$ ). When  $\beta=0.5$  and for  $O_R$  ranging between 0.00% to 25.00% the slabs with opening showed decreasing values of total ultimate load with respect to solid slab. While beyond  $O_R$  of 25.00%, a clear increase in the total ultimate load is noticed as shown in **Figs. 15**. Also these figures reveal that the increase in  $UL_R$  and  $TL_R$  values are increased with increasing the value of  $\beta$ . For values of  $\beta$  (0.5, 1.0, 1.5 and 2.0), the  $UL_R$  values are 3.73, 4.73, 5.33 and 5.73 respectively for opening ratio ( $O_R$ )=60%. While  $TL_R$  values are 1.49, 1.89, 2.13 and 2.29 respectively for the same above values.

## 6. CONCLUSIONS

1. From the experimental results for simply supported square slabs, the cracking and ultimate uniform loads were decreased as opening ratio ( $O_R$ ) is increased from 0.00% to 25.00%. The maximum percentage decrease in cracking and ultimate loads were 31.82% and 12.17% compared to the control solid slab for opening ratios ( $O_R$ ) of 11.11% and 6.25% respectively. Beyond the values of  $O_R=11.11%$  and 6.25%, the percentages decrease in cracking load and ultimate uniform load were decreased respectively.



2. For opening ratio ( $O_R$ )=25.00%, the ultimate uniform load capacity is approximately similar to the value obtained for the control solid slab. This might be due concentration of the uniform load near supports which leads to increase the slab stiffness.
3. The maximum and minimum cracking to ultimate uniform load ratios ( $w_{cr}/w_u$ ) were 0.507 and 0.386 for the control solid slab and for the slab with opening ratio ( $O_R$ ) of 11.11% respectively.
4. From the experimental results, it can be noticed that the opening ratio ( $O_R$ ) has a significant effect on deflection values through the entire range of loading starting from crack and up to ultimate load. For slabs of  $O_R$  (2.78%, 6.25% and 11.11%), the load-deflection curve showed a significant increase in deflection compared to control solid slab. While for slabs with  $O_R$  of (17.36% and 25.00%), the load-deflection curve showed a slight decrease in deflection values compared to the control solid slab.
5. At a load level of 130 kN/m<sup>2</sup> which is about 85% of ultimate uniform load capacity of the control slab, it is found that the maximum percentage increase in deflection is 39.13% for slab of  $O_R$ =2.78% at location of 250 mm from supports. While, the maximum percentage decrease in deflection is 11.47% for slab of  $O_R$ =17.36% at location of 175 mm from supports.
6. Based on the theoretical analysis for simply supported slabs it is found that for opening ratio ( $O_R$ ) ranging between 0.00% and 25.00% a decrease in ultimate uniform load for a slab with central opening relative to the ultimate uniform load for a solid slab ratio ( $UL_R$ ) is occurred. The maximum decrease in  $UL_R$  was 0.889 for  $O_R$ =6.25%. While beyond  $O_R$  of 25.0%, a significant increase in ultimate uniform load is occurred. Also according to the theoretical analysis it is found that the total ultimate load for a slab with central opening relative to the total ultimate load for a solid slab ratio ( $TL_R$ ) is decreased as  $O_R$  is increased.
7. According to the theoretical analysis for clamped ends slab, it is found that as  $O_R$  is increased, both  $UL_R$  and  $TL_R$  are increased for all values of ( $\beta$ ) which represents the ratio of the negative resistance moment at clamped ends to the positive resistance moment along the positive yield lines. Except when the value of  $\beta$ =0.5 within  $O_R$  ranging between 0.00% to 25.00% the  $TL_R$  is decreased. While beyond  $O_R$  of 25.00%, a clear increase in the total ultimate load is noticed. Also, it is found that as the value of  $\beta$  is increased, both  $UL_R$  and  $TL_R$  values are increased.

## REFERENCES

- ACI Committee 318, 2014, *Building Code Requirements for Reinforced Concrete and Commentary (ACI 318-14 and ACI 318R-14)*, American Concrete Institute, Detroit.
- ASTM Designation C 494/C 494M-01b, 2001, *Standard Specifications for Chemical Admixture for Concrete*, Annual Book of ASTM Standards, American Society for Testing and Materials, Philadelphia, Pennsylvania.
- BS 8110-1, 1997, *Structural Use of Concrete, Code of Practice for Design and Construction*, British Standards Institution, London, PP 163.
- Iraqi Specification No. 5, 1984, *Portland Cement*, Baghdad.
- Iraqi Specification No. 45, 1984, *Natural Sources for Gravel That is Used in Concrete and Construction*, Baghdad.
- Khayat, K. H., and Ghezal, A., 1999, *Utility of Statistical Models in Proportioning Self-Compacting Concrete*, Proceedings, RILEM, International symposium on Self-Compacting Concrete, Stockholm, PP. 345-359.



- Mota, M. C., and Kamara, M., 2006, *Floor Openings in Two-Way Slabs*, Concrete International Journal, Vol.28, No.7, PP. 33-66.
- Nagamoto, N., and Ozawa, K., 1997, *Mixture Properties of Self-Compacting High-Performance Concrete*, Proceedings, Third CANMET, ACI International Conferences on Design and Materials and Recent Advances in Concrete Technology, SP-172, V. M. Malhotra, American Concrete Institute, Farmington Hills, Mich., PP. 623-637.
- Taljsten, B., Lundqvist, J., Enochsson, O., Rusinowski, P., and Olofsson, T., 2006, *CFRP Strengthened Openings in Two-way Concrete Slabs—An Experimental and Numerical Study*, Construction and Building Materials, PP. 810-826.
- The European Guidelines for Self-Compacting Concrete, 2005, *Specification, Production and Use*. PP. 28.
- Wang, C. K., Salmon, C. G., and Pincheira, J. A., 2007, *Reinforced Concrete Design*, Seventh Edition, John Wiley and Sons, New York, PP. 948.

## NOMENCLATURE

$d$  = depth of steel bars from top fiber of the section

$E_s$  = modulus of elasticity of steel bars

$f'_c$  = cylindrical compressive strength of self-compacting concrete

$f_y$  = yield stress of steel reinforcement

$f_u$  = ultimate strength of steel reinforcement

$L$  = dimension of square slab.

$l$  = projected length of yield line.

$LSP$  = limestone powder

$m$  = resistance moment per unit length

$O_R$  = opening ratio

$P_u$  = total ultimate load

$RC$  = reinforced concrete

$SCC$  = self- compacting concrete

$TL_R$  = ratio of total ultimate load for a slab with opening to total ultimate load for a solid slab

$UL_R$  = ratio of ultimate uniform load for a slab with opening to ultimate uniform load for a solid slab

$w_{cr}$  = cracking load

$WE$  = external work

$WI$  = internal work

$w_u$  = ultimate uniform load

$Z$  = dimension of central square opening.

$\beta$  = ratio of negative resistance moment at fixed end to positive resistance moment along positive yield lines

$\Delta$  = unit displacement

$\rho$  = steel ratio of section

$\theta$  = rotation along yield line

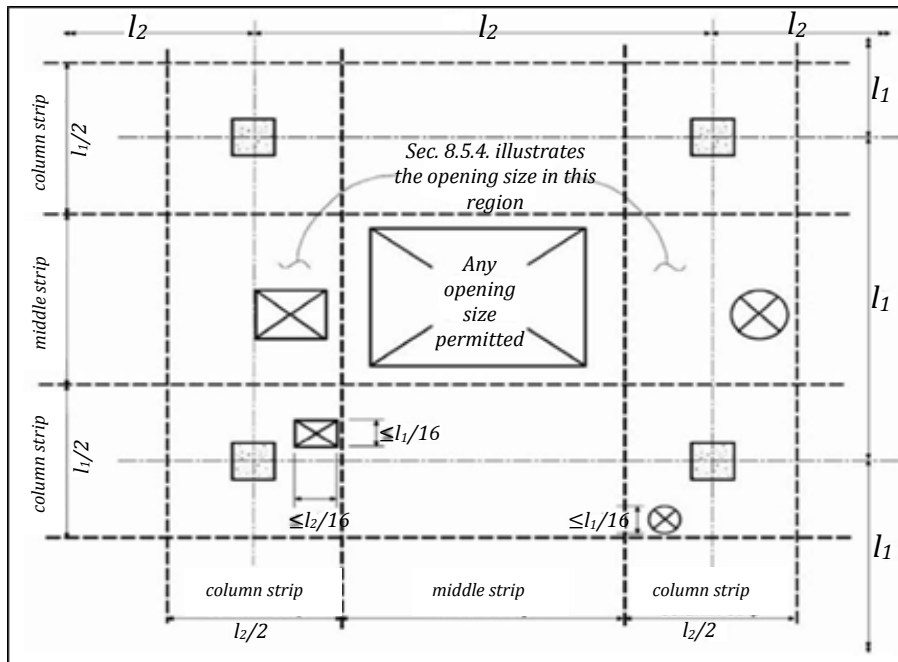


Figure 1. Suggested opening size and location in flat slab according to the *ACI-318, 2014 Code*.

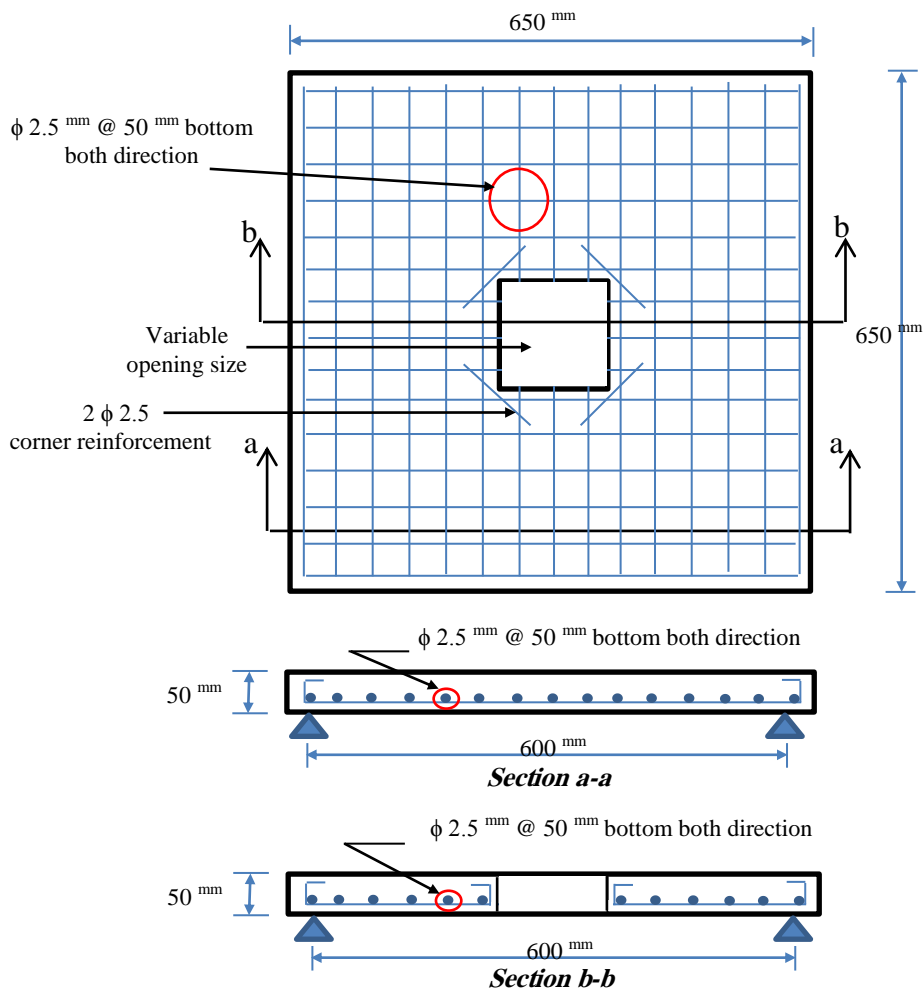
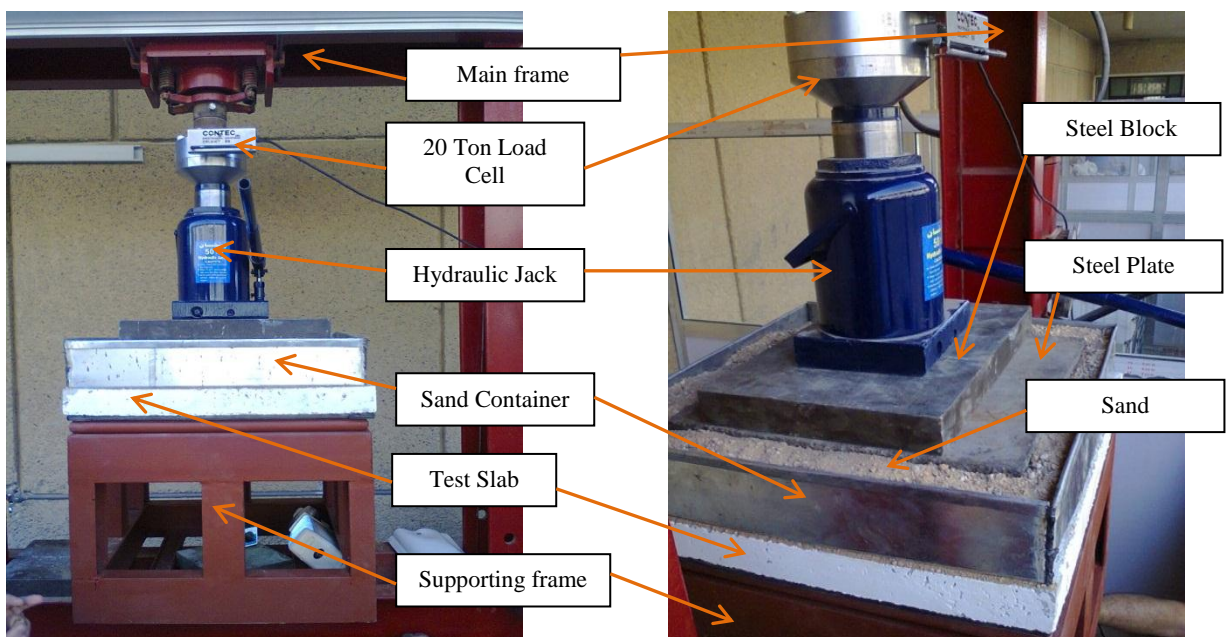


Figure 2. Layout of a typical tested slab.



**Figure 3.** Molds fabrication and reinforcement meshes for some tested slabs.



**Figure 4.** Setup of a typical tested slab.

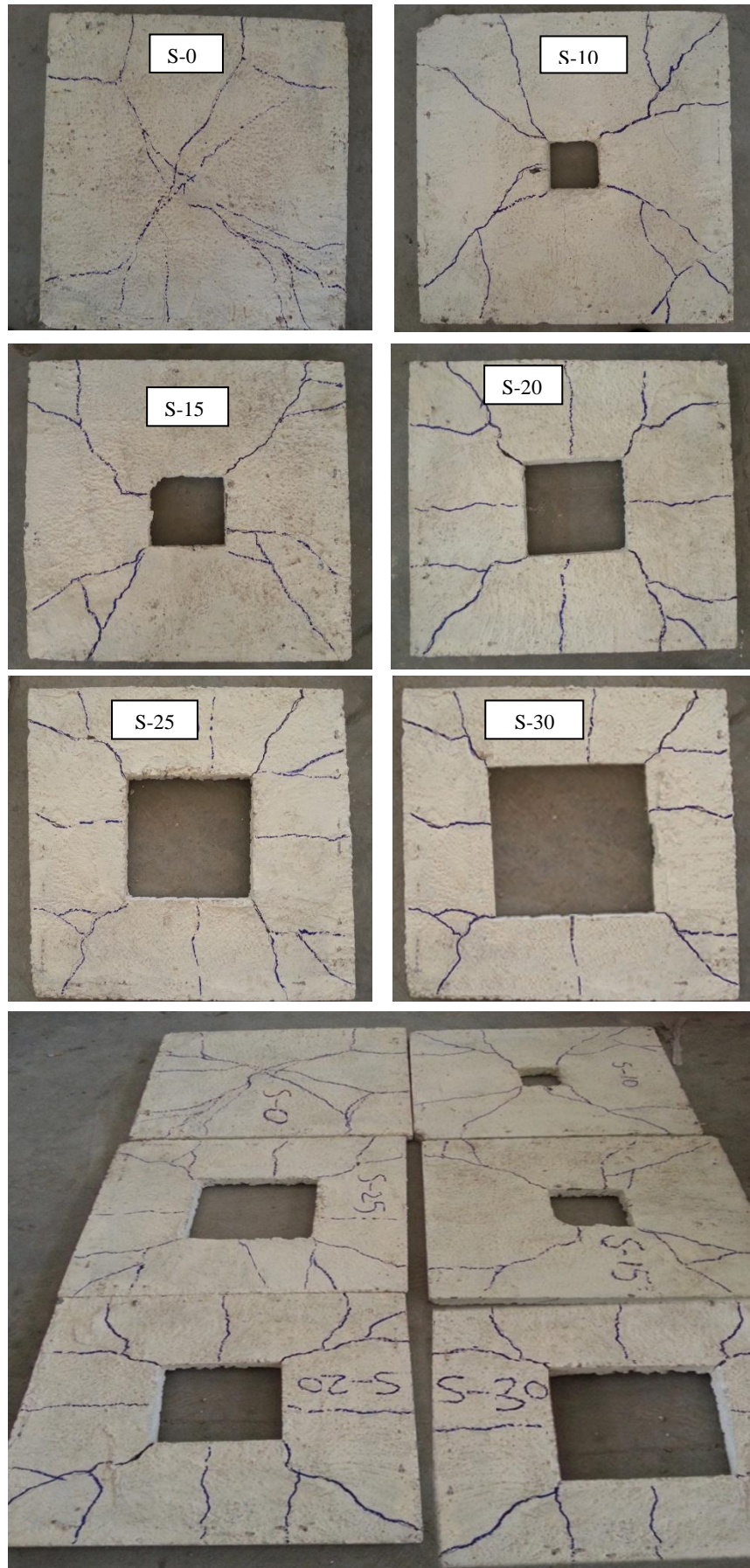


**Figure 5.** Bottom face of tested slabs after failure.

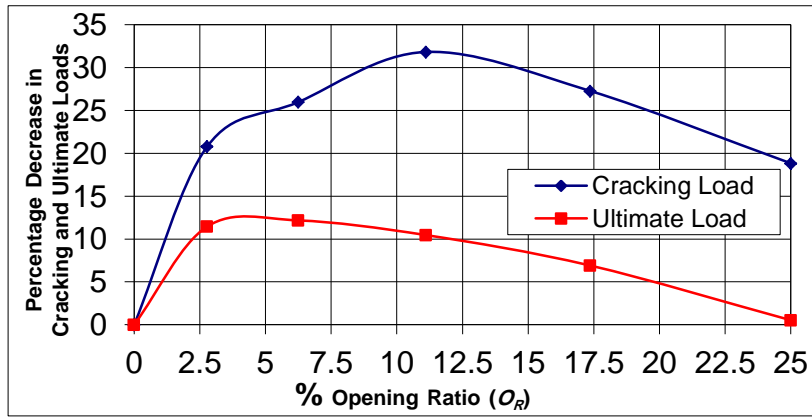


Figure 6. Percentage decrease in cracking and ultimate uniform loads with varying opening ratios.

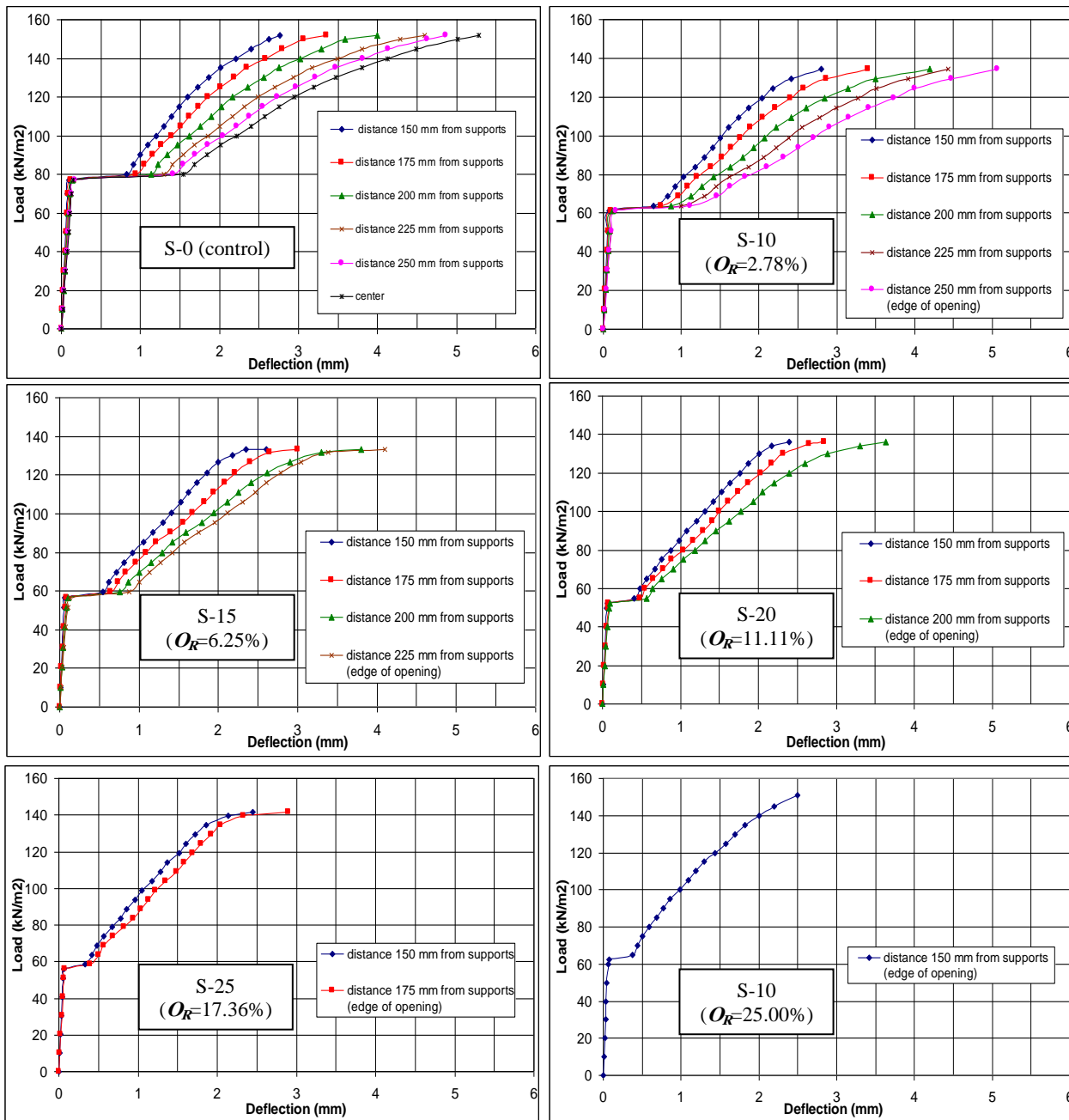


Figure 7. Load-deflection curves for tested slabs at different dial gauge locations.

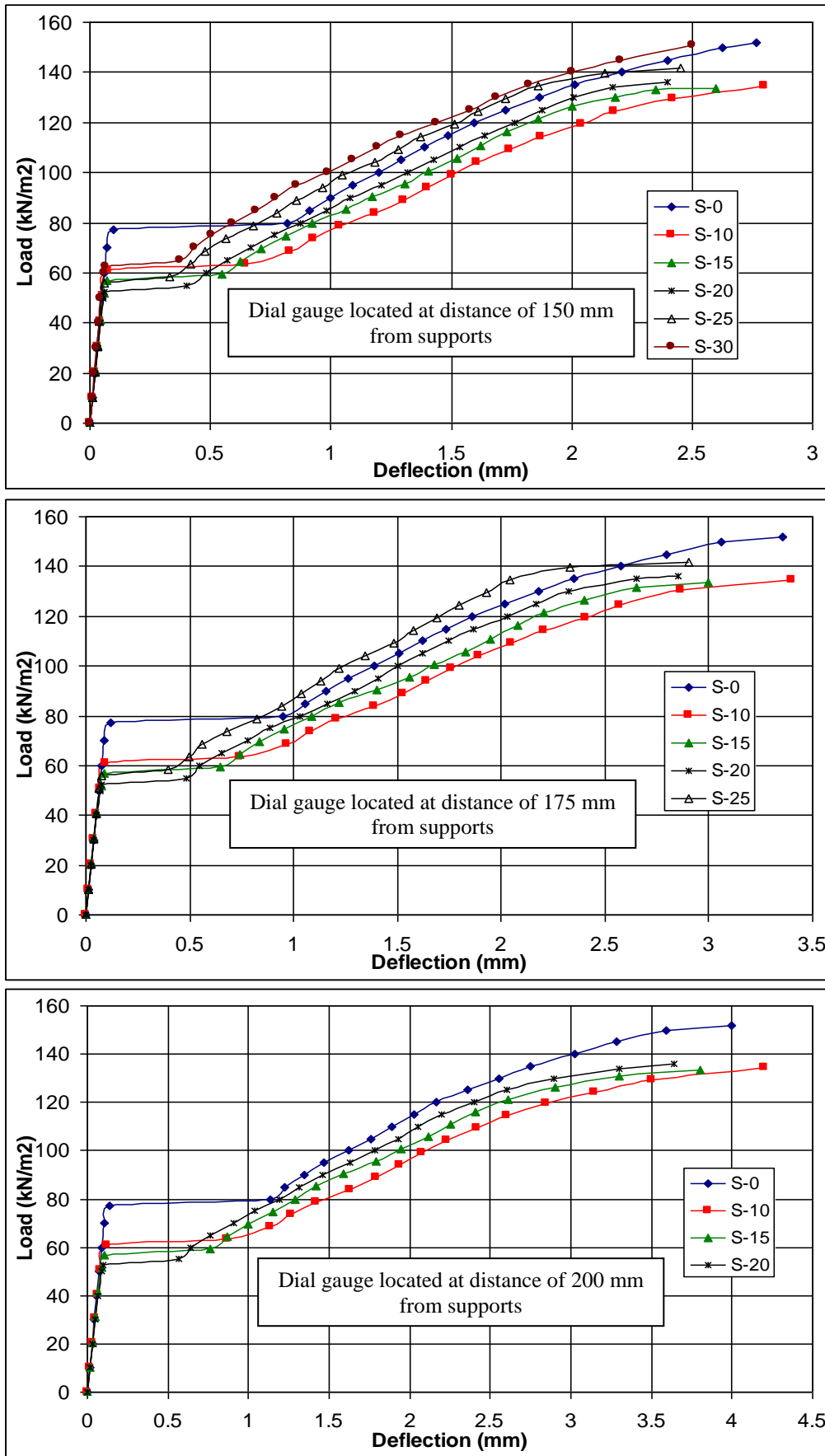


Figure 8. Load-deflection curves for tested slabs recorded by same dial gauge locations.

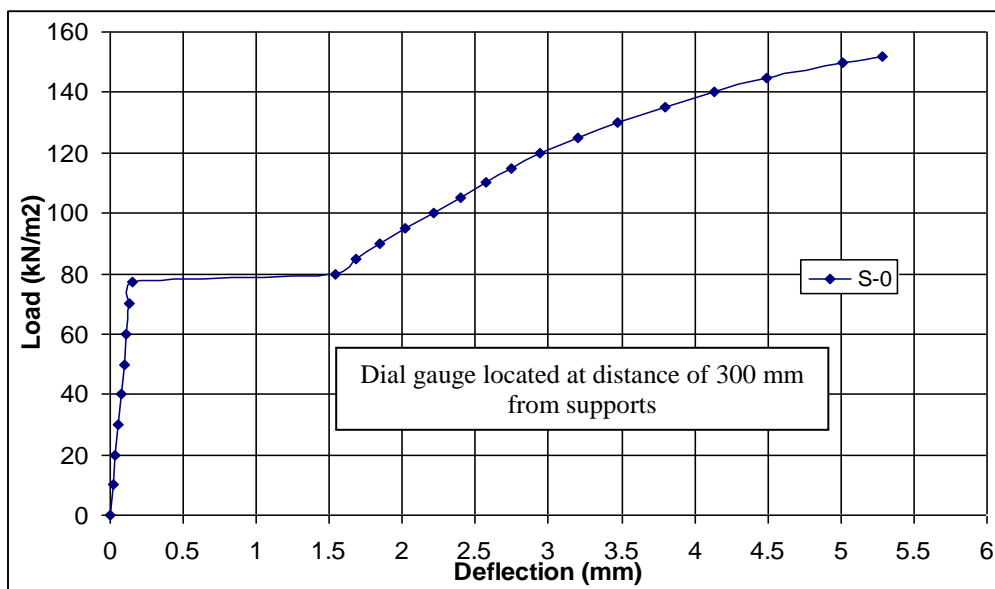
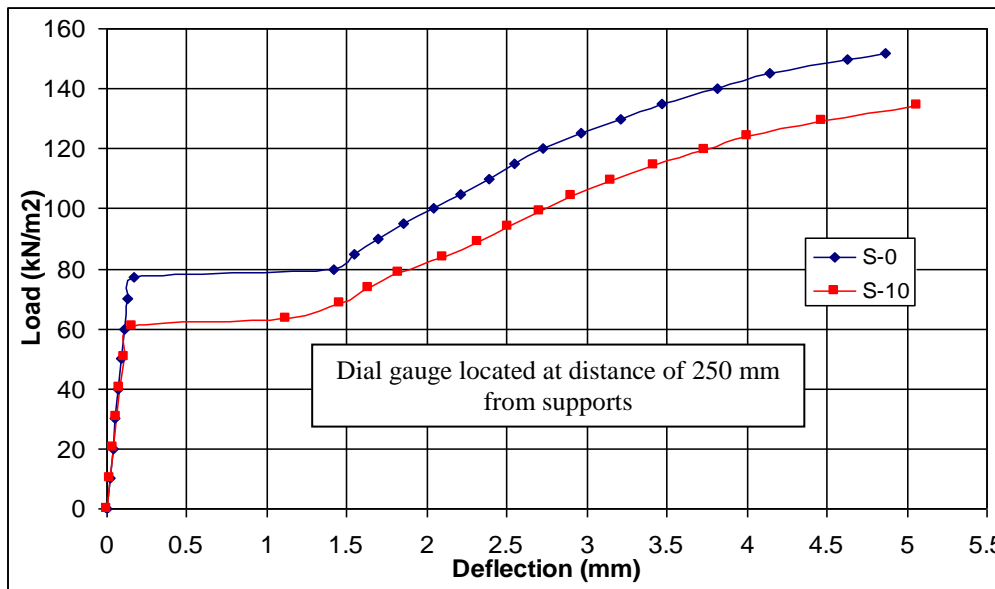
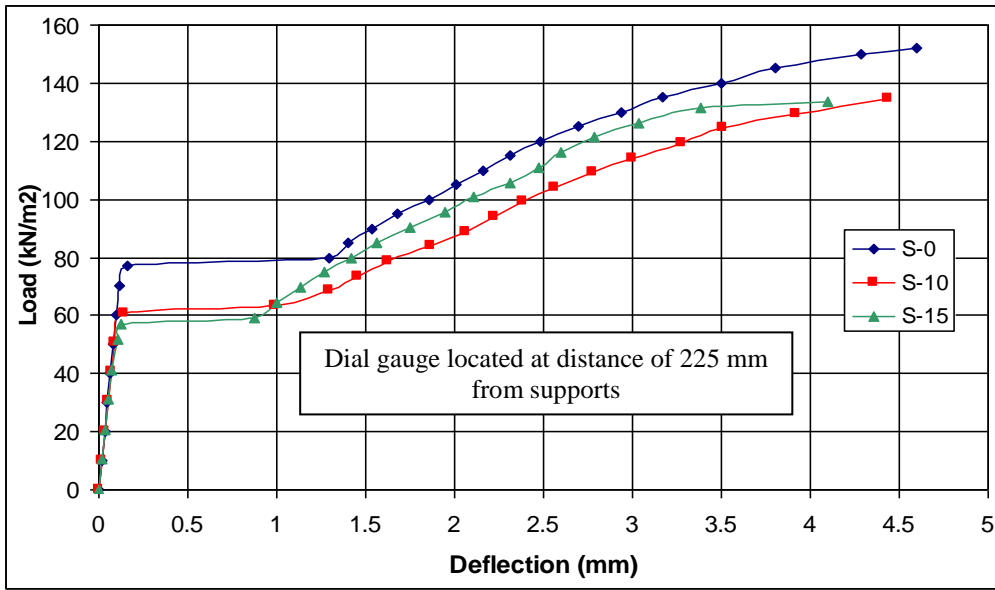


Figure 8. Continue.

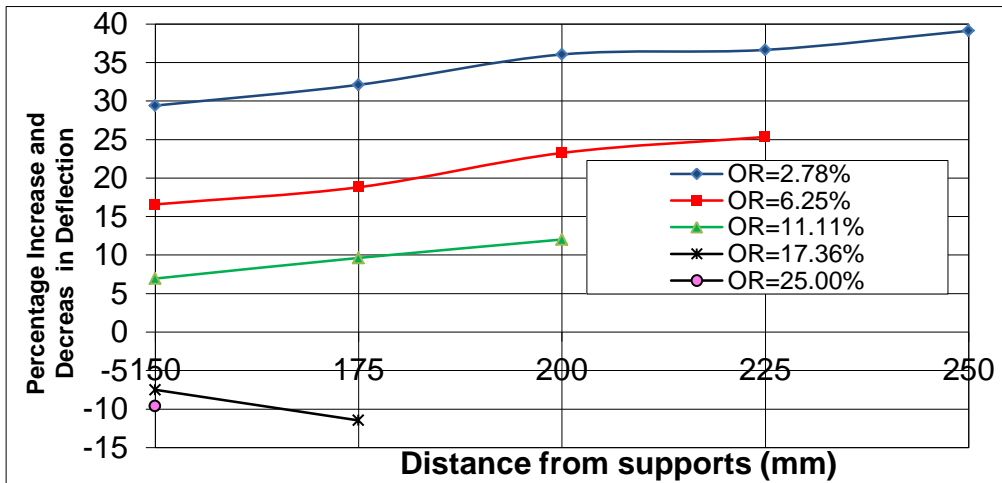


Figure 9. Percentage increase and decrease in deflection with respect to distance of recorded deflection from supports corresponding to a load level of 130 kN/m<sup>2</sup>.

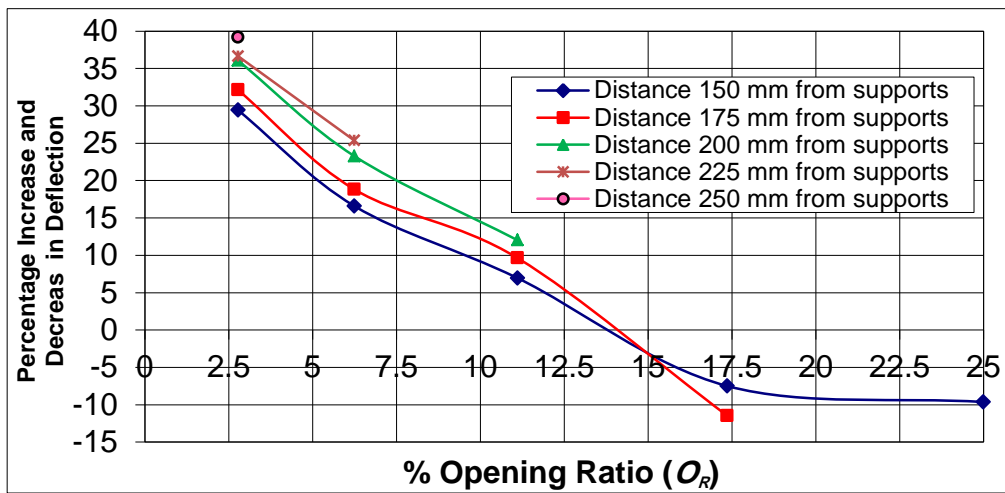


Figure 10. Percentage increase and decrease in deflection with respect to opening ratios corresponding to a load level of 130 kN/m<sup>2</sup>.

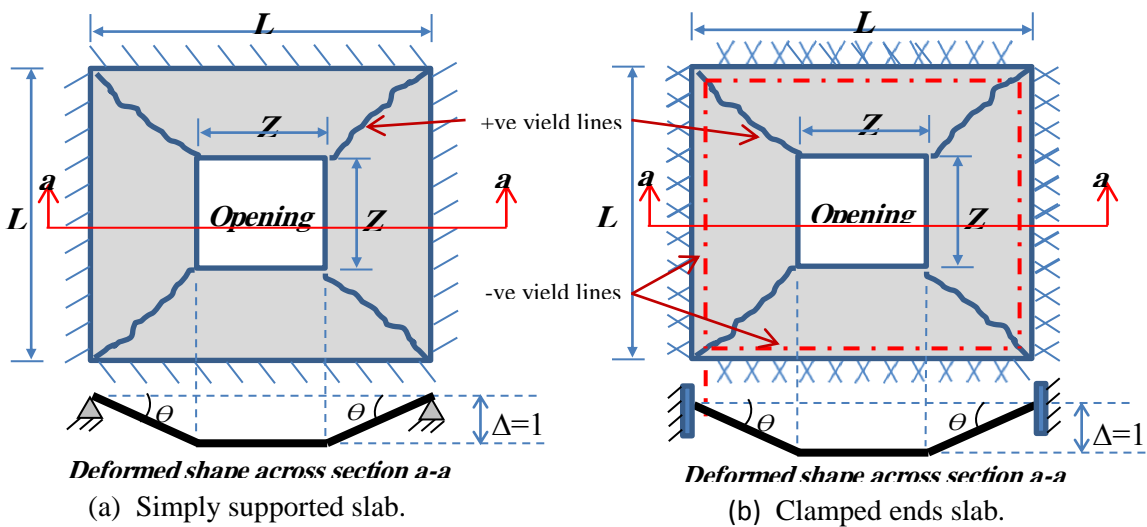


Figure 11. Yield lines and deformations of simply supported and clamped ends square slabs with central square opening.

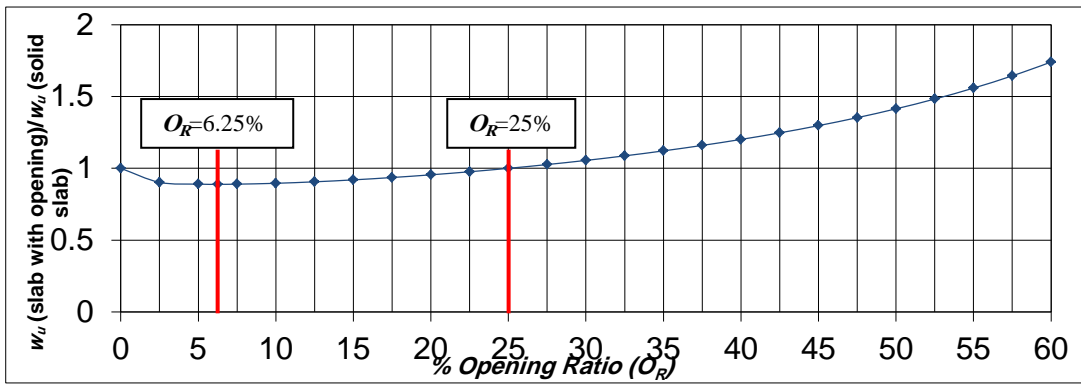


Figure 12. Effect of opening ratio on ultimate uniform load of simply supported slabs.

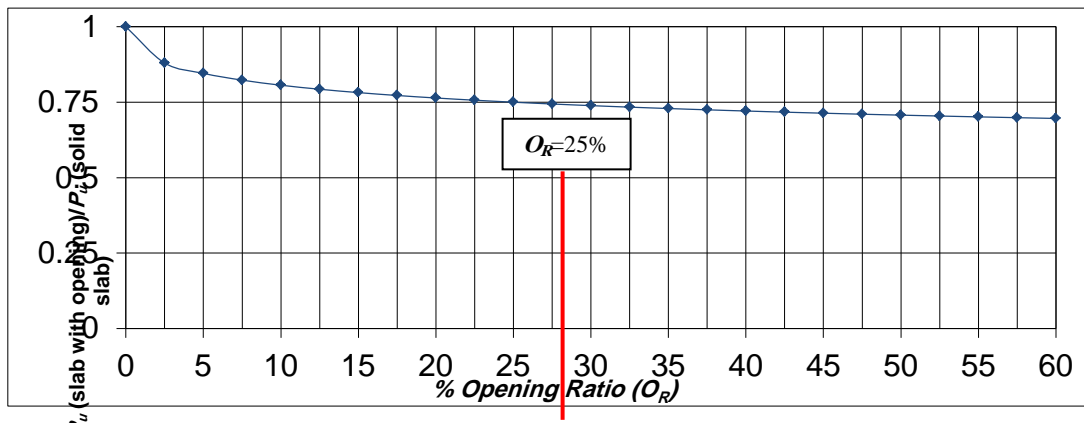


Figure 13. Effect of opening ratio on total ultimate load of simply supported slabs.

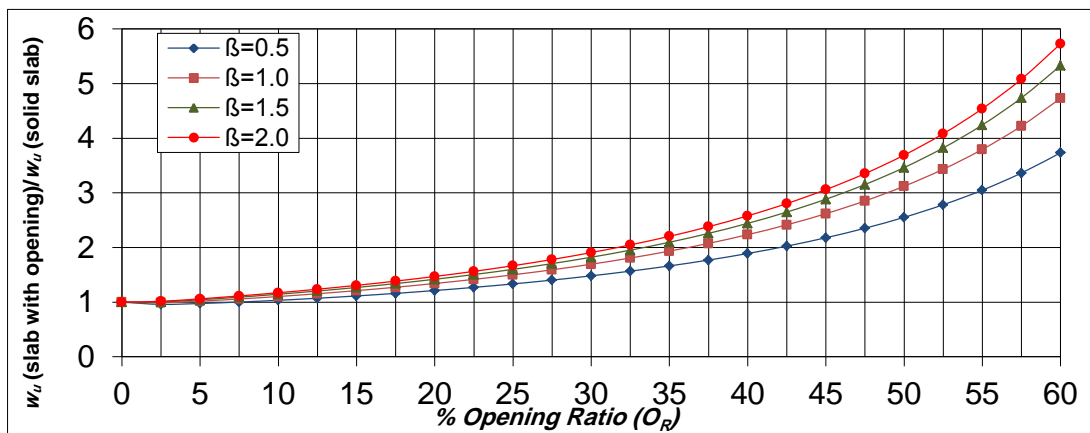


Figure 14. Effect of opening ratio on ultimate uniform load of clamped ends slabs.

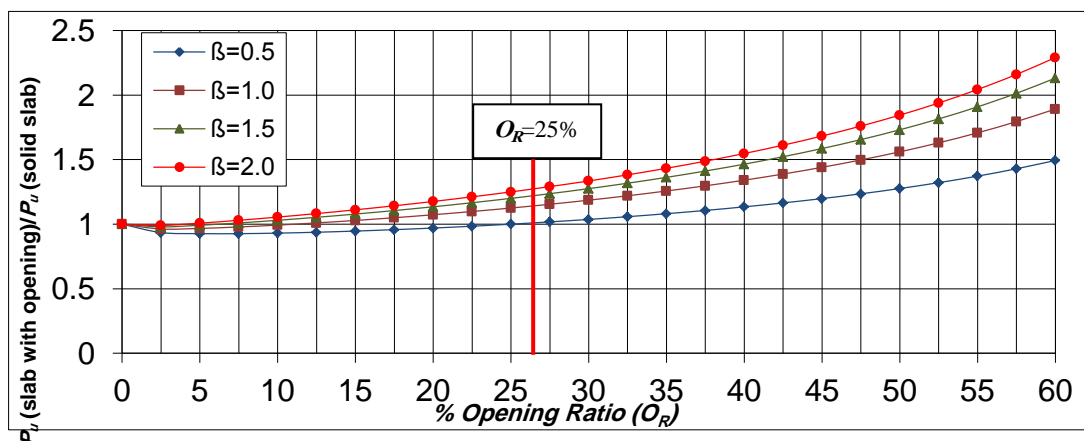


Figure 15. Effect of opening ratio on total ultimate load of clamped ends slabs.

**Table 1.** Properties of tested slabs.

Slab designation		Slab dimensions center to center of supports (mm)	Opening dimensions (mm)	% Opening ratio( $O_R$ )
S-0	control	600 x 600	-	0.00
S-10		600 x 600	100 x 100	2.78
S-15		600 x 600	150 x 150	6.25
S-20		600 x 600	200 x 200	11.11
S-25		600 x 600	250 x 250	17.36
S-30		600 x 600	300 x 300	25.00

$$\% \text{ Opening ratio } (O_R) = \frac{\text{Area of opening}}{\text{Area of soild slab}} \times 100$$

**Table 2.** Mix properties for SCC used in this research

Cement ( $\text{Kg/m}^3$ )	Sand ( $\text{Kg/m}^3$ )	Gravel ( $\text{Kg/m}^3$ )	LSP ( $\text{Kg/m}^3$ )	Water (litter/ $\text{m}^3$ )	Superplasticizer (litter/ $\text{m}^3$ )
371	845	792	199	185	4

**Table 3.** Dial gauges location .

Slab designation		Opening dimensions (mm)	No. of dial gauges used	Location of dial gauge No.1 from supports (mm)	Location of dial gauge No.2 from supports (mm)	Location of dial gauge No.3 from supports (mm)	Location of dial gauge No.4 from supports (mm)	Location of dial gauge No.5 from supports (mm)	Location of dial gauge No.6 from supports (mm)
S-0	control	-	6	150	175	200	225	250	300 (center)
S-10		100 x 100	5	150	175	200	225	250 (edge of opening)	N.A
S-15		150 x 150	4	150	175	200	225 (edge of opening)	N.A	N.A
S-20		200 x 200	3	150	175	200 (edge of opening)	N.A	N.A	N.A
S-25		250 x 250	2	150	175 (edge of opening)	N.A	N.A	N.A	N.A
S-30		300 x 300	1	150 (edge of opening)	N.A	N.A	N.A	N.A	N.A

N.A Not applicable



**Table 4.** Experimental cracking and ultimate loads results .

Slab designation		% Opening ratio( $O_R$ )	Cracking Load $w_{cr}$ (kN/m <sup>2</sup> )	% Decrease in cracking load	Ultimate load $w_u$ (kN/m <sup>2</sup> )	% Decrease in ultimate load	$w_{cr}/w_u$
S-0	control	0.00	77.0	control	152.0	control	0.507
S-10		2.78	61.0	20.78	134.6	11.45	0.453
S-15		6.25	57.0	25.97	133.5	12.17	0.427
S-20		11.11	52.5	31.82	136.1	10.46	0.386
S-25		17.36	56.0	27.27	141.5	6.91	0.396
S-30		25.00	62.5	18.83	151.2	0.53	0.413

$$\% \text{ Decrease} = \frac{W_{\text{control slab}} - W_{\text{slab with opening}}}{W_{\text{control slab}}} \times 100$$

**Table 5.** Deflections coresponding to a load level of 130 kN/m<sup>2</sup>.

Slab designation	A	AA	B	BB	C	CC	D	DD	E	EE	F	FF
S-0 control	1.87	control	2.18	control	2.58	control	2.92	control	3.22	control	3.47	control
S-10 ( $O_R=2.78\%$ )	2.42	+29.41	2.88	+32.11	3.51	+36.05	3.99	+36.64	4.48	+39.13	N.A	N.A
S-15 ( $O_R=6.25\%$ )	2.18	+16.58	2.59	+18.81	3.18	+23.26	3.66	+25.34	N.A	N.A	N.A	N.A
S-20 ( $O_R=11.11\%$ )	2.00	+6.95	2.39	+9.63	2.89	+12.02	N.A	N.A	N.A	N.A	N.A	N.A
S-25 ( $O_R=17.36\%$ )	1.73	-7.49	1.93	-11.47	N.A	N.A	N.A	N.A	N.A	N.A	N.A	N.A
S-30 ( $O_R=25.00\%$ )	1.69	-9.63	N.A	N.A								

- A Deflection (mm) recorded at location of 150 mm from supports
- B Deflection (mm) recorded at location of 175 mm from supports
- C Deflection (mm) recorded at location of 200 mm from supports
- D Deflection (mm) recorded at location of 225 mm from supports
- E Deflection (mm) recorded at location of 250 mm from supports
- F Deflection (mm) recorded at location of 300 mm from supports

$$XX \text{ Percentage increase or decrease in deflection with respect to control slab} = \frac{\text{def. control slab} - \text{def. slab with opening}}{\text{def. control slab}} \times 100$$

(+) Sign for increasing in deflection and (-) sign for decreasing in deflection  
 N.A Not applicable

**Table 6.** Effect of opening ratio on ultimate loads results for simply supported slabs.

Slab designation	% Opening ratio( $O_R$ )	Experimentally		Experimentally		Theoretically		$\frac{ULR (Exp.)}{ULR (Theo.)}$	$\frac{TLR (Exp.)}{TLR (Theo.)}$
		$w_u$ (kN/m <sup>2</sup> )	$P_u$ (kN)	$ULR$	$TLR$	$ULR$ Applying Eq. (9)	$TLR$ Applying Eq. (10)		
S-0 control	0.00	152.0	54.72	1.0000	1.0000	1.0000	1.0000	1.0000	1.0000
S-10	2.78	134.6	47.11	0.8855	0.8609	0.8999	0.8750	0.9840	0.9839
S-15	6.25	133.5	45.06	0.8783	0.8235	0.8889	0.8333	0.9881	0.9882
S-20	11.11	136.1	43.55	0.8954	0.7959	0.8999	0.8000	0.9950	0.9949
S-25	17.36	141.5	42.10	0.9309	0.7694	0.9350	0.7727	0.9956	0.9957
S-30	25.00	151.2	40.82	0.9947	0.7460	1.0000	0.7500	0.9947	0.9947

$$ULR = \frac{w_u (\text{slab with opening})}{w_u (\text{solid slab})}, TLR = \frac{P_u (\text{slab with opening})}{P_u (\text{solid slab})}, P_u = w_u \times \text{area of slab}$$